Biochimica et Biophysica Acta 1807 (2011) 518–528

Contents lists available at ScienceDirect

Biochimica et Biophysica Acta

journal homepage: www.elsevier.com/locate/bbabio

Energy transfer in an LH4-like light harvesting complex from the aerobic purple photosynthetic bacterium *Roseobacter denitrificans*

Dariusz M. Niedzwiedzki [a,*], Marcel Fuciman [d], Harry A. Frank [d], Robert E. Blankenship [a,b,c]

[a] *Photosynthetic Antenna Research Center, Campus Box 1138, Washington University in St. Louis, St. Louis, MO 63130, USA*
[b] *Department of Biology, Washington University in St. Louis, MO 63130, USA*
[c] *Department of Chemistry, Washington University in St. Louis, MO 63130, USA*
[d] *Department of Chemistry, University of Connecticut, U-3060, 55 North Eagleville Road, Storrs, CT 06269–3060, USA*

ARTICLE INFO

Article history:
Received 11 February 2011
Received in revised form 8 March 2011
Accepted 11 March 2011
Available online 16 March 2011

Keywords:
LH4
LH2
Carotenoids
Bacteriochlorophyll
Transient absorption
Light harvesting

ABSTRACT

A peripheral light-harvesting complex from the aerobic purple bacterium *Roseobacter (R.) denitrificans* was purified and its photophysical properties characterized. The complex contains two types of pigments, bacteriochlorophyll (BChl) *a* and the carotenoid (Car) spheroidenone and possesses unique spectroscopic properties. It appears to lack the B850 bacteriochlorophyll *a* Q_y band that is typical for similar light-harvesting complex 2 antennas. Circular dichroism and low temperature steady-state absorption spectroscopy revealed that the B850 band is present but is shifted significantly to shorter wavelengths and overlaps with the B800 band at room temperature. Such a spectral signature classifies this protein as a member of the light-harvesting complex 4 class of peripheral light-harvesting complexes, along with the previously known light-harvesting complex 4 from *Rhodopseudomonas palustris*. The influence of the spectral change on the light-harvesting ability was studied using steady-state absorption, fluorescence, circular dichroism, femtosecond and microsecond time-resolved absorption and time-resolved fluorescence spectroscopies. The results were compared to the properties of the similar (in pigment composition) light-harvesting complex 2 from aerobically grown *Rhodobacter sphaeroides* and are understood within the context of shared similarities and differences and the putative influence of the pigments on the protein structure and its properties.

1. Introduction

Light-harvesting complexes (LHC) are essential elements of the photosynthetic apparatus in all photosynthetic organisms. LHCs absorb incident light and transfer the excitation energy to the reaction center where it is converted into chemical energy in a series of electron-transfer steps. Despite having the same functionality among many different photosynthetic organisms, LHCs are not structurally unified and diverge into many subgroups having different structural properties and pigment composition [1].

Purple bacteria produce two general types of LHCs, the light harvesting complex 1 (LH1), closely associated with the reaction center (RC) and light-harvesting complex 2 (LH2), peripherally arranged around LH1-RC. The structure of the LH2 antenna complex has been determined for *Rhodopseudomonas (Rps.) acidophila* strain 10050 and *Phaeospirillum (Phs.) molischianum* bacterial species using X-ray crystallography. Both complexes were determined to ~2.5 Å resolution; however the LH2 from *Rps. acidophila* was later improved to 2.0 Å [2–5]. The LH2 complex from *Rps. acidophila* forms a circular structure consisting of nine identical protein subunits formed by heterodimers of polypeptide chains denoted α and β oriented across the photosynthetic membrane. The protein subunits form a double ring with inner and outer diameters of 36 Å and 68 Å. Each of the subunits accommodates three bacteriochlorophylls *a* (BChl *a*) molecules and one Car, rhodopin glucoside. Rhodopin glucoside spans the space between the α and β polypeptide pairs and is in close contact with a pair of the strongly coupled BChl *a* molecules (B850). The B850 BChls are oriented perpendicular to the membrane plane and form a ring of 9 pairs of BChl molecules. The minimum distances between B850 BChls are 3.66 Å within dimers and 3.74 Å between molecules from neighboring dimers. The monomeric BChl *a* molecules (B800) are oriented parallel with the membrane plane and positioned between β–polypeptides [2–4]. The LH2 complex from *Phs. molischianum* has a similar circular structure with eight α/β subunits forming inner and outer rings with dimensions of 31 Å and 62 Å with 8 dimers of B850 BChl pigments and 8 monomeric B800 BChls. Different structural packing in both complexes affects the distance of closest approach between the B850 BChls which are 3.54 Å (within dimer) and 3.63 Å (between pairs). The LH2 complex from *Phs. molischianum* contains also 8 lycopene molecules. Lycopene is a carotenoid that adopts in the LH2 complex of *Phs. molischianum* a similar orientation as rhodopin glucoside in the *Rps. acidophila* LH2 complex despite its different structure [5].

* Corresponding author. Tel.: +1 314 935 8483; fax +1 314 935 4925.
E-mail address: niedzwiedzki@wustl.edu (D.M. Niedzwiedzki).

0005-2728/$ – see front matter © 2011 Elsevier B.V. All rights reserved.
doi:10.1016/j.bbabio.2011.03.004

The spectroscopic properties of the LH2 antenna complexes are determined by their structure. The Q_y absorption band of BChls absorbing at 800 nm originates from the monomeric, widely-spaced (21 Å between Mg atoms) B800 BChls, while the band appearing at 850 nm is associated with the closely-spaced ring (9 Å between Mg atoms) of the strongly coupled dimeric B850 molecules. Specific spacing, contiguity of the molecules in the rings, and alignment of the transition dipole moments lead to excitonic coupling that shifts absorption of both molecular arrangements to longer wavelength to different degrees compared to the absorption of individual BChl *a* molecules.

Several purple bacteria species express "anomalous" peripheral light harvesting antenna complexes under stressed conditions such as low light or low temperature. Complexes discovered in *Rps. acidophila* strain 7050 and in *Rps. cryptolactis* have the B850 band blue shifted to 820 nm. Due to its spectroscopic character, this complex is referred to as B800–B820 or LH3. Its crystal structure has been determined with a resolution of 3.0 Å for *Rps. acidophila* strain 7050 and revealed only very small differences in comparison to the "standard" LH2 structure from strain 10050 [6]. It was concluded that the observed blue-shift of the BChl bands is caused by minor differences in the primary structure of the apoprotein which affects the hydrogen bonds (H-bonds) between BChls and the protein [6]. A spectrally similar complex B800–B830 was also found in *Chromatium (Chr.) purpuratum* [7]. In response to low light conditions, another purple bacterium, *Chr. vinosum* produces a complex with a suppressed B850 band in its absorption spectrum and is also called the B800 complex [8]. Similarly, *Rhodopseudomonas palustris* expresses a complex with a greatly reduced B850 band under low light condition. This complex has been called both B800 and LH4. A high-resolution crystal structure of this LH4 is still not available; however, a 7.5 Å resolution density map was published by Hartigan et al. [9]. Such resolution is too low to draw definitive conclusions about pigment organization in the structure. Nevertheless, using a combination of spectroscopic and biochemical methods, the authors concluded that LH4 is built from eight α/β peptide pairs and each subunit contains four BChls *a* (32 in total) in contrast to three in the "standard" LH2 [9].

In this work, we present studies on the low-light peripheral light-harvesting complex from the purple aerobic anoxygenic phototrophic bacterium *Roseobacter (R.) denitrificans* (known also as *Erythrobacter sp.* strain OCh114), as a candidate for another LH4 complex. This complex was initially described by Shimada et al. in the 1990s as a B806 complex due to the BChl Q_y band absorbance at that wavelength. Since then, only a very basic spectroscopic characterization of this protein has been performed [10,11]. We used several different optical spectroscopic techniques including steady state absorption, fluorescence, circular dichroism, femtosecond and microsecond time-resolved transient absorption, and nanosecond time-resolved fluorescence at both room and cryogenic temperatures to reveal how these spectroscopic properties influence light harvesting and excitation transfer in this unusual complex.

2. Materials and methods

2.1. Cell growth

R. denitrificans strain OCh114 was grown under aerobic conditions on Difco Marine Broth 2216 media. A small volume of liquid culture was used to inoculate 1 L media, split into 4 equal flasks, which were closed with foam stoppers. The cultures were placed in the dark, in an incubator at 30 °C and continuously shaken. The cells were harvested after 7 days of growth when they were assumed to be in a stationary stage.

2.2. Preparation of the peripheral LH antenna complex

The cells were resuspended in 20 mM Tris buffer (pH = 8.0) and the membranes were released by ultrasonication process and then pelleted by centrifugation at 250,000*g* for 2 h. Subsequently, the pellet was resuspended in 20 mM Tris buffer (pH = 8.0) ($OD_{800nm} \approx 20$) and mixed with lauryldimethylamine-oxide (LDAO) to a final concentration of 1% for 20 minutes at 4 °C. The mixture was then centrifuged at 250,000*g* for 1 h to separate insoluble material. Further purification of the complexes was carried out using an anion exchange chromatographic column (Q Sepharose High Performance, GE Healthcare) equilibrated with 20 mM Tris–HCl buffer (pH 8) with 0.1% LDAO by applying a linear gradient of NaCl between 0 and 500 mM. The protein-containing fraction eluted with 250–300 mM NaCl. For low temperature measurements, the sample was resuspended in a 50:50 (vol./vol.) glycerol:buffer solution.

2.3. Steady-state absorption, fluorescence and CD spectroscopy

Room temperature steady-state absorption spectra were recorded using a Perkin Elmer Lambda 950 spectrophotometer. Room temperature fluorescence emission and fluorescence excitation spectra were recorded using a Photon Technology International fluorometer. The 10 K absorption spectrum was recorded using Varian Cary-50 spectrophotometer equipped with a liquid helium cryostat Janis-100. The 10 K fluorescence emission and fluorescence excitation spectra were recorded using a Fluorolog-3 fluorometer from Jobin-Yvon Horiba equipped with the same cryostat. In all cases, fluorescence was monitored at a right-angle relative to the excitation. Excitation and emission monochromator slits were set to a bandpass of 4 nm. Fluorescence excitation spectra were corrected using a calibrated reference diode. Circular dichroism was measured using a Jasco 815 CD spectrometer at room temperature with 1 nm spectral resolution.

2.4. Time-correlated single-photon-counting spectroscopy

Fluorescence lifetime measurements were done using a time-correlated single-photon-counting (TCSPC) system of a Jobin-Yvon Horiba Fluorolog 3 equipped with a Single Photon Counting Controller FluoroHub 2.0 (J-Y Horiba) and a pulsed NanoLed-370 diode (as excitation light source), with excitation at 370 nm and a pulse duration less than 1.3 ns. The sample emission was monitored at the maximum of the emission peak.

2.5. Femtosecond time-resolved transient absorption spectroscopy

Transient pump–probe absorption experiments were carried out using Helios, a femtosecond transient absorption spectrometer (Ultrafast Systems, LCC), coupled to a femtosecond laser system previously described in detail [12,13]. The system is based on a Spitfire-50 fs, Ti:sapphire amplifier with pulse stretcher and compressor (Spectra-Physics) pumped at 1 kHz repetition rate by Evolution 15, Q-switched Nd:YLF laser (Coherent) and seeded by pulses from Tsunami, mode-locked Ti:sapphire oscillator (Spectra-Physics), that is pumped by Millenia VsJ, diode-pumped Nd:YVO_4 CW visible laser (Spectra Physics). Output pulses, with center wavelength of 800 nm, energy of 600 μJ/pulse, ~50 fs duration, and 1 kHz repetition were split into two beams by a beam splitter. Ninety percent of the signal was sent to OPA-800C optical parametric amplifier (Spectra-Physics) to generate a pump beam. The remaining 10% was used to derive probe pulses. A white light continuum probe 450–800 nm in the visible region (VIS), and 850–1450 nm in the near infrared (NIR) was generated by a 3 mm Sapphire plate. A charge-coupled detector S2000 with a 2048 pixel array from Ocean Optics was used as a detector in the VIS range. In the NIR, a 512 pixel array SU-LDV high resolution InGaAs Digital Line Camera from Sensors Unlimited was used. The pump and probe beams were overlapped at the sample at the magic-angle (54.7°) polarization. The signals were averaged over 5 seconds. The samples were pumped into the 0–0 vibronic band of the $S_0(1^1A_g^-) \rightarrow S_2(1^1B_u^+)$ steady-state absorption

spectrum of Car. The energy of the pump beam was set to 1 μJ/pulse in a spot size of 1 mm diameter corresponding to intensity between 3.0 and 5.4×10^{14} photons/cm^2 per pulse (depending on excitation wavelength). The optical densities (OD) of the samples were adjusted to 2.0–2.5 at the excitation wavelength in a 1 cm cuvette; however, measurements were performed in 2 mm path length cuvettes. The samples were mixed continuously using a magnetic micro-stirrer to prevent photo-degradation. Low temperature (10 K) transient absorption measurements were done using a Janis-100 liquid helium cryostat and 4 mm cuvette. The integrity of the samples was checked by taking a steady-state absorption spectrum before and after every experiment.

2.6. Microsecond time-resolved transient absorption spectroscopy

Microsecond transient absorption experiments were performed on the samples in a 1-cm path length cuvette at room temperature and at 77 K using Edinburgh Instruments (EI) LP920-K/S flash photolysis spectrometer equipped with a Tektronix TDS 3012 C digital oscilloscope. Excitation pulses were delivered from an Opotek Vibrant 355 tunable laser system consisting of 10 Hz Nd:YAG laser (Quantel), second and third harmonic generators and optical parametric oscillator (Opotek). Energy of the excitation beam was set to ~2 mJ/pulse, equal to a photon density of $5.4–6.4\times10^{15}$ photons/cm^2 depending on the excitation wavelength. A 450 W xenon arc lamp was used as a probe light source. The excitation (laser) and probe (white light) beams were configured in a standard 90° cross-beam geometry. The probe light was dispersed in a symmetrical Czerny–Turner monochromator (TMS300) and focused onto either a Hamamatsu R2658 photomultiplier detector (kinetic mode) or an ICCD camera (IStar with DH720-18H-13 CCD head) (spectral mode). Transient absorption signals were averaged 60–100 times. Sample integrity was checked by taking steady-state absorption spectra before and after every experiment. Low temperature (77 K) triplet transient spectra and lifetime measurements of the pigments in the peripheral light harvesting complex from *R. denitrificans* were performed using an Optistat^{DN} cryostat from Oxford Instruments fitted to EI LP920-K/S spectrometer as described above. Oxygen from solution was removed by applying ten freeze–pump–thaw cycles under a vacuum of 1 mTorr as described previously [14].

2.7. Transient absorption data analysis and fitting

Group velocity dispersion (GVD) of the transient absorption spectra was corrected using Surface Explorer (v.1.1) software (Ultrafast Systems LCC) by building a dispersion correction curve from a set of initial times of transient signals obtained from single wavelength fits of representative kinetics. The number of principal kinetic components in the data sets was determined by singular value decomposition (SVD) using the same software. Global fitting analysis of the transient absorption data sets was performed using ASUfit 3.0, program provided by Dr. Evaldas Katilius at Arizona State University, with modifications. The full width at half maximum (FWHM) of a temporal response function was assumed to be 120 fs for all the measurements and was used as a fixed parameter in fitting. Carotenoid triplet lifetimes were obtained by fitting the single wavelength kinetics to a monoexponential decay function.

3. Results

3.1. Steady-state absorption spectra

The steady-state absorption spectra, converted to 1-T, where T is transmittance, fluorescence excitation profiles and fluorescence emission of the peripheral light harvesting complex from *R. denitrificans* taken in buffer (20 mM Tris–HCl (pH 8), 0.1% LDAO) at RT and in glycerol/buffer (50/50, vol./vol.) at 10 K, are shown in Fig. 1A and B, respectively. In addition, the absorption spectrum of spheroidenone taken at RT in toluene is also given. The absorption spectrum of the complex shows features attributed to both BChl *a* (Soret, Q_x and B800 bands) and spheroidenone (broad featureless S_0 ($1^1A_g^-$) → S_2($1^1B_u^+$) band in 500–600 nm range). The room temperature absorption spectrum does not show any evidence of the BChl *a* B850 band related with the ring of the closely associated BChls. Thus, from a spectroscopic point of view, this LH complex is equivalent to the LH4 obtained from low-light adapted *Rps. palustris*. However, the 10 K absorption spectrum with enhanced resolution of the Q_y band clearly reveals another BChl *a* band with maximum at ~820 nm. This is strong evidence that the Q_y bands originating from monomeric and dimeric BChl rings are degenerate and are practically indistinguishable at RT. This finding is also confirmed by fluorescence. The emission spectrum follows with long-wavelength absorption band while the temperature is lowered. However, low temperature does not significantly improve the resolution of the Car band, which remains broad, with only slightly better resolved visible vibronic bands. Interestingly, the RT absorption spectrum of this complex closely resembles the low temperature absorption spectrum of the LH4 from *Rps. palustris* (excluding the Car band) [15]. However, the 10 K spectrum mimics the RT absorption of the LH3 (B800–B820) complex from *Rps. acidophila* [16,17]. At this point we do not know the structure of this complex and therefore, the combination of spectroscopic properties makes it difficult to assign it to either the LH3 or LH4 class. Nevertheless, based on similarities in the RT absorption spectrum in the NIR range with that from the LH4 complex from *Rps. palustris* and the peripheral antenna complex studied here, we categorize the complex as an LH4 type and hence, this name will be used in the following text.

3.2. Energy transfer efficiency

The Car-to-BChl excitation energy transfer efficiencies (EET) were determined by taking the ratio of amplitudes of the spheroidenone peaks in the fluorescence excitation and 1-T profiles for three different wavelengths and averaged. The spectral profiles were normalized to 1

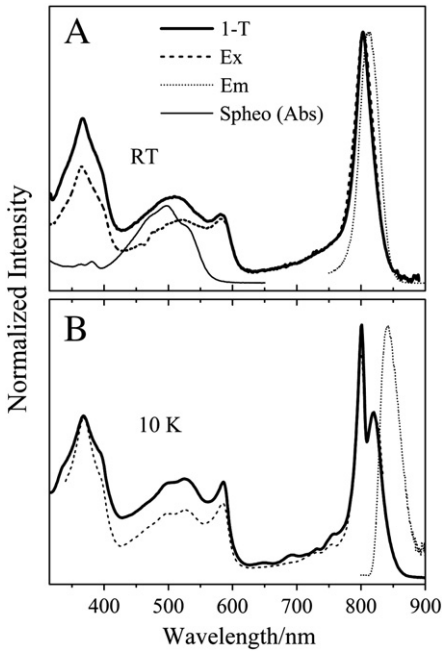

Fig. 1. Steady-state absorption, fluorescence excitation and fluorescence emission spectra of the LH4 antenna complex from *R. denitrificans*. The spectra were taken at room temperature (RT) (A) and at 10 K (B). The steady-state absorption of spheroidenone taken at RT in toluene is also shown.

at 800 nm (RT) or at 820 nm (10 K) where it was assumed that the energy transfer will be equal to 100%. The EET value is 73 ± 7% at RT and 69 ± 1% at 10 K.

3.3. Circular dichroism

The results of circular dichroism of the LH4 from *R. denitrificans* measured at RT in buffer are shown in Fig. 2. The spectrum contains a series of pronounced negative and positive features, associated either with BChl *a* (300–400 nm, 550–610 nm and 790–850 nm ranges) or with spheroidenone (400–550 nm range). The CD band in the 800 nm range has zero crossing point at 808 nm and is red shifted by 5 nm with respect to the absorption maximum.

3.4. BChl a fluorescence lifetime in LH4

Fig. 3 shows BChl *a* fluorescence decay kinetics in the LH4 from *R. denitrificans* measured at RT and at 10 K. The traces were recorded at the maximum of the fluorescence band (812 nm at RT and 825 nm at 10 K). The instrument response function (IRF) is also shown. In both cases the kinetics were deconvoluted by a combination of the IRF and one (10 K) or two (RT) exponential decays. The lifetimes obtained from fitting are 630 ps (74%) and 3 ns (26%) at RT and 1.8 ns (100%) at 10 K. The component with lifetime of 3 ns found in the RT results is probably associated with free BChl *a*, which has a comparable fluorescence lifetime [14].

3.5. Transient absorption of spheroidenone

Transient absorption spectra of spheroidenone in toluene, taken at various delay times after the excitation pulse, are shown in Fig. 4A and B. In the visible range, the spectra exhibit negative broad features at early time delays, which is associated with the combination of an immediate bleaching of the strongly allowed $S_0(1^1A_g^-) \rightarrow S_2(1^1B_u^+)$ electronic transition and stimulated emission from the $S_2(1^1B_u^+)$ state. Subsequently, there is a build-up of transient absorption signal with maximum at 600 nm (Fig. 4A). This band persists for several picoseconds and was assigned to the $S_1(2^1A_g^-) \rightarrow S_n$ transition [12,18–24]. In the NIR spectral region (Fig. 4B) the transient absorption spectra are dominated by a strong transition with maximum around 1050 nm. This band is known to be associated with the $S_2(1^1B_u^+) \rightarrow S_n$ electronic transition and decays completely within 500 fs. Subsequently, a weak and broad transient absorption band appears and persists for several picoseconds. This band was assigned previously to the $S_1(2^1A_g^-) \rightarrow S_2(1^1B_u^+)$ transition. In this case, it is not fully recorded due to detector spectral response range limitation. Applying the singular value decomposition (SVD) procedure allowed us to estimate numbers of significant principal component in the transient absorption data sets. For the data sets from the VIS range, three principal components were obtained, and for NIR two. Subsequently, global fitting of the data sets was performed with numbers of fitting components obtained from SVD, using an unbranched, unidirectional decay path model (A → B → C → D → …). In this model back-reactions are ignored on the assumption that the energy losses are large enough that the reverse reaction rates are negligible [25]. The spectral profiles obtained from this kind of fitting of TA data sets are termed evolution associated difference spectra (EADS). The fitting was done for both VIS and NIR data sets and the results are shown in Fig. 4C and D. Fig. 4E and F shows the representative kinetics extracted from the VIS and NIR data sets (symbols) accompanied with the fits (solid lines) obtained from global fitting. The kinetics were taken at 587 nm (maximum of the $S_1(2^1A_g^-) \rightarrow S_n$ transition) and at the 1065 nm ($S_2(1^1B_u^+) \rightarrow S_n$ transient band).

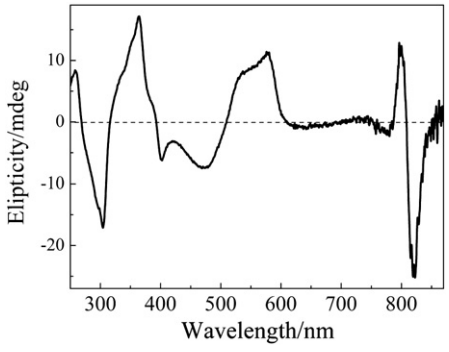

Fig. 2. Circular dichroism spectrum of the LH4 from *R. denitrificans*. The spectrum was taken at room temperature on a sample with OD_{800} adjusted to 0.5.

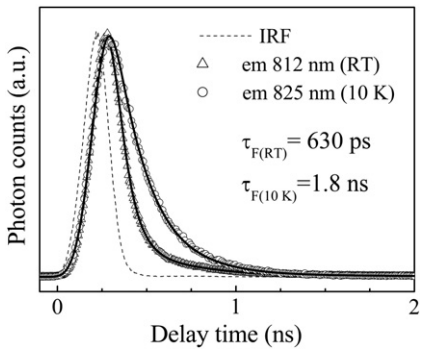

Fig. 3. Room temperature and 10 K BChl *a* fluorescence decay kinetics in the LH4 from *R. denitrificans* recorded using time correlated single photon counting spectroscopy. The kinetics were measured at the maximum of the fluorescence spectrum and are normalized for comparison purposes. The dashed line represents the instrument response function (IRF). The fluorescence lifetimes obtained from kinetic deconvolution are indicated in the figure.

3.6. Transient absorption of the LH4 at RT (VIS, NIR)

Transient absorption spectra of the LH4 light harvesting complex from *R. denitrificans* taken at room temperature in buffer in VIS and NIR ranges are shown in Fig. 5. The sample was excited at the $S_0(1^1A_g^-) \rightarrow S_2(1^1B_u^+)$ band of spheroidenone (520 nm), close to the expected 0–0 vibronic band. The transient spectra show an instantaneous onset of bleaching of the $S_0(1^1A_g^-) \rightarrow S_2(1^1B_u^+)$ spheroidenone absorption in the 450–500 nm range accompanied with a strong, broad positive band with maximum at 1050 nm (Fig. 5A). This band is associated with the $S_2(1^1B_u^+) \rightarrow S_n$ transition of spheroidenone and shows substantial similarity to its counterpart measured in toluene. In addition, immediate bleaching of the BChl *a* Q_y band at 822 nm is also visible. The $S_2(1^1B_u^+) \rightarrow S_n$ transition of spheroidenone decays within a few hundred femtoseconds and is coupled with partial recovery of bleaching of the ground state absorption. Subsequently, the broad, positive spectral feature with maximum at 607 nm appears and covers the entire 550–750 nm range. The spectral profiles obtained from sequential decay fitting of the TA data sets are shown in Fig. 5C and D and were done separately for the VIS and the NIR spectral ranges. The fitting procedure gave satisfactory results with four kinetic components in both cases. Fig. 5E–G shows representative kinetics extracted from VIS and NIR data sets (circles) accompanied with fits (solid lines) from global fitting. The kinetics were taken at the maximum of the $S_1(2^1A_g^-) \rightarrow S_n$ transition (607 nm), at 827 nm (BChl*a* Q_y bleaching) and at 1030 nm (maximum of the $S_2(1^1B_u^+) \rightarrow S_n$ transient band).

3.7. Transient absorption of the LH4 at 10 K (VIS, NIR)

Transient absorption spectra of the LH4 from *R. denitrificans* taken at 10 K in VIS and NIR ranges upon excitation of the $S_0(1^1A_g^-) \rightarrow S_2(1^1B_u^+)$ transition of the Car are shown in Fig. 6A and B. Similar to the RT data, the spectra show an instantaneous onset of bleaching of the Car ground state absorption in 450–500 nm (Fig. 6A) and a strong,

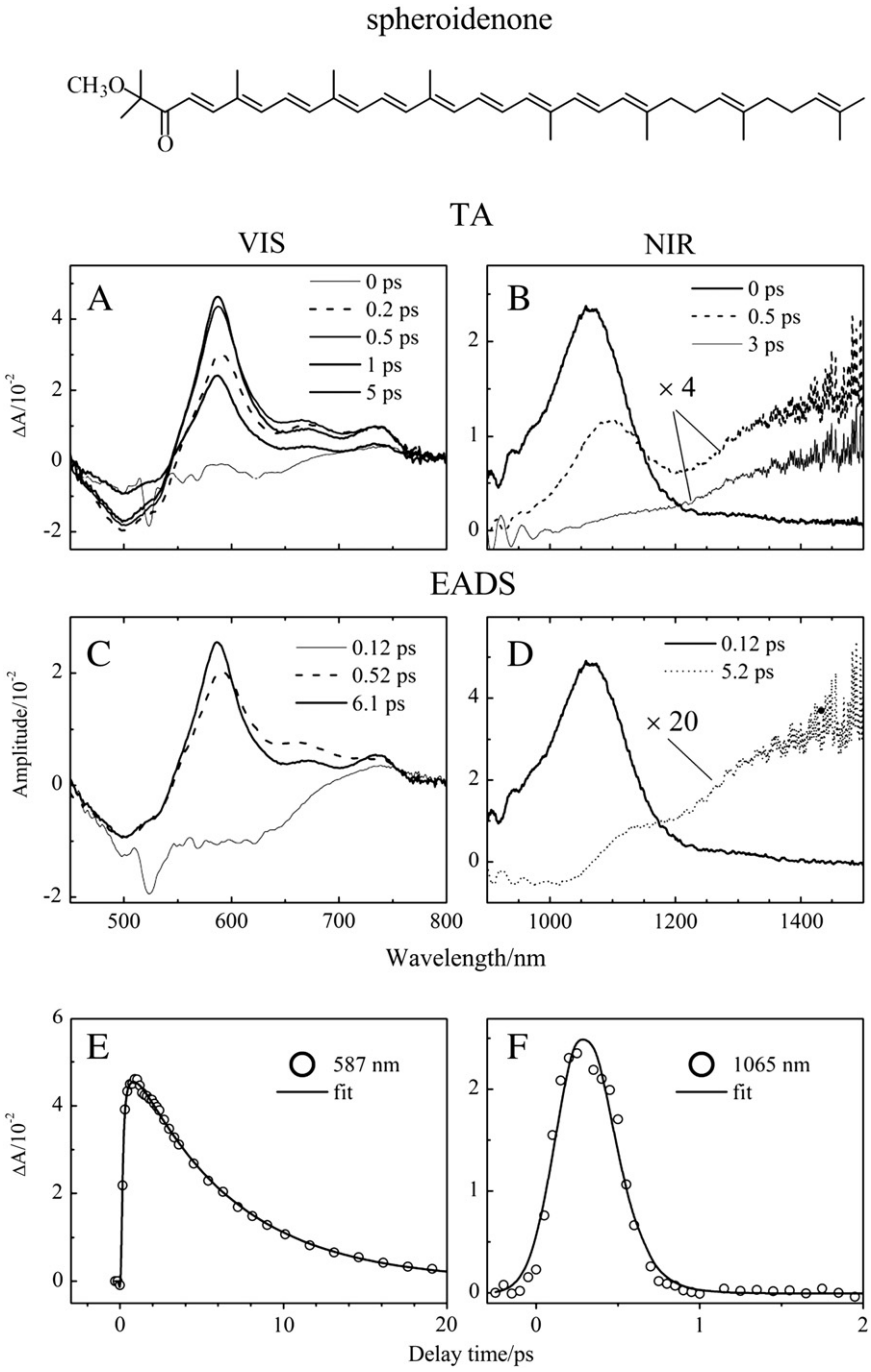

Fig. 4. (A, B) Room temperature transient absorption spectra (TA) of spheroidenone taken at different delay times in visible (VIS) and near-infrared (NIR) ranges in toluene. The Car was excited at 520 nm; (C, D) The results of global fitting of the transient absorption data sets using a sequential decay path (EADS); (E, F) the representative kinetics for VIS and NIR ranges extracted from the transient absorption data sets (symbols) with the corresponding fits obtained from global fitting analysis (solid lines).

broad positive band in the NIR range (Fig. 6B). Low temperature did not significantly improve the spectral band resolution; however it caused a noticeable shift of the transient bands. The $S_2(1^1B_u^+) \rightarrow S_n$ transition of spheroidenone is shifted by 60 nm to 1090 nm, the $S_1(2^1A_g^-) \rightarrow S_n$ transient band has maximum at 625 nm compared to 610 nm at RT. In addition, the band at 965 nm is more apparent at 10 K. Global fitting results are given in Fig. 6C and D. The lifetimes of the kinetic components are in agreement with their RT counterparts. Fig. 6E–F represent kinetics extracted from the VIS and the NIR data sets (circles) with the fits (solid lines) obtained from global fitting. The kinetics were taken at the maximum of the $S_1(2^1A_g^-) \rightarrow S_n$ transition (624 nm) and at 970 nm.

3.8. Triplet–singlet (T–S) spectra and triplet dynamics of the LH4

Transient absorption spectra of the LH4 from *R. denitrificans* taken at different delay times in the microsecond time domain at RT and at 10 K are shown in Fig. 7A–D. The spectra were recorded upon excitation of the $S_0(1^1A_g^-) \rightarrow S_2(1^1B_u^+)$ spheroidenone band (at 550 nm) (Fig. 7A and C) and the Q_x band of BChl *a* (590 nm) (Fig. 7B and D). Regardless of excitation wavelength or temperature, the spectra are almost identical in terms of shape and consist of a strong $T_1 \rightarrow T_n$ absorptive band centered at 600 nm. The band maximum shifts slightly to longer wavelengths (607 nm) when temperature is lowered. The $T_1 \rightarrow T_n$ transient band is accompanied by bleaching of the spheroidenone ground state. A closer

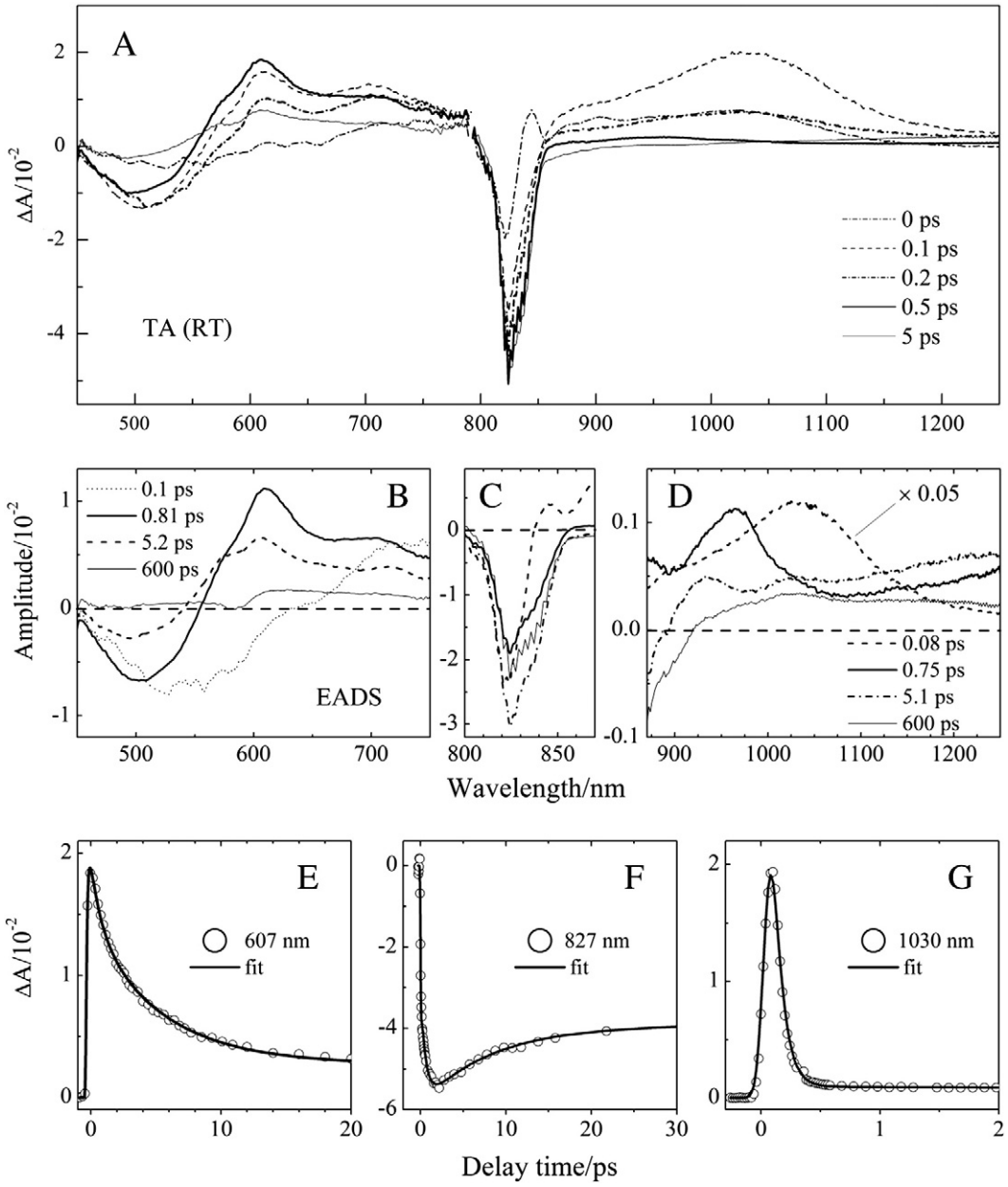

Fig. 5. (A) Room temperature transient absorption spectra (TA) of the LH4 from *R. denitrificans*. The spectra were taken at different delay times and are shown in combined VIS-NIR range. The LH4 complex was excited at 520 nm; (B–D) The results of global fitting of transient absorption datasets using sequential decay path (EADS). Fitting was done separately for VIS and NIR ranges; (E–G) The representative kinetics for VIS and NIR ranges extracted from the transient absorption data sets (circles) with corresponding fits obtained from global fitting analysis (solid lines).

view reveals also small negative bands at 800 (RT) and 820 nm (10 K), corresponding well to the positions of the Q_y bands of BChl *a* in RT and low temperature steady-state absorption spectra. Fig. 7E and F show the triplet decay kinetics recorded at the maximum of the spheroidenone $T_1 \rightarrow T_n$ band at both temperatures. The kinetics were normalized for comparison purposes. Fitting of RT kinetics using monoexponential decay gave lifetimes of 3.3 and 3.6 μs for 550 nm and 590 nm excitations, respectively, and 6.9 and 7.0 μs for the experiments at 10 K. The results clearly show that temperature significantly affects the Car triplet lifetime.

4. Discussion

The low-temperature steady-state absorption spectrum (Fig. 1B) clearly shows the presence of the Q_y band originating from the tightly bound ring of BChls molecules. Even if this transition is perfectly covered by the B800 band at RT, low temperature shifts it by ~20 nm to longer wavelengths and both transitions become resolved. It is known that the B850 band is sensitive to temperature changes. Upon lowering the temperature, the protein contracts and distances between the B850 molecules decrease and a stronger excitonic coupling is induced [26]. As a consequence, the splitting between the energy levels of the B850 exciton states increases. Spectrally, this is observed as a red shift of the B850 band, associated with the transition to the low energy level of the exciton [26]. The position of the Q_y band of the dimeric BChl *a* in this LH4 complex at RT can be deducted from the CD spectrum shown in Fig. 2. Previous studies demonstrated that the CD signal associated with the B800 band is barely visible or equal to zero at RT [26]. However, the LH4 CD spectrum shows a strong CD signal in the vicinity of 800 nm (with zero crossing at 808 nm) that must be associated with the "B850" band. It is also known that the zero crossing point does not coincide with the absorption maximum

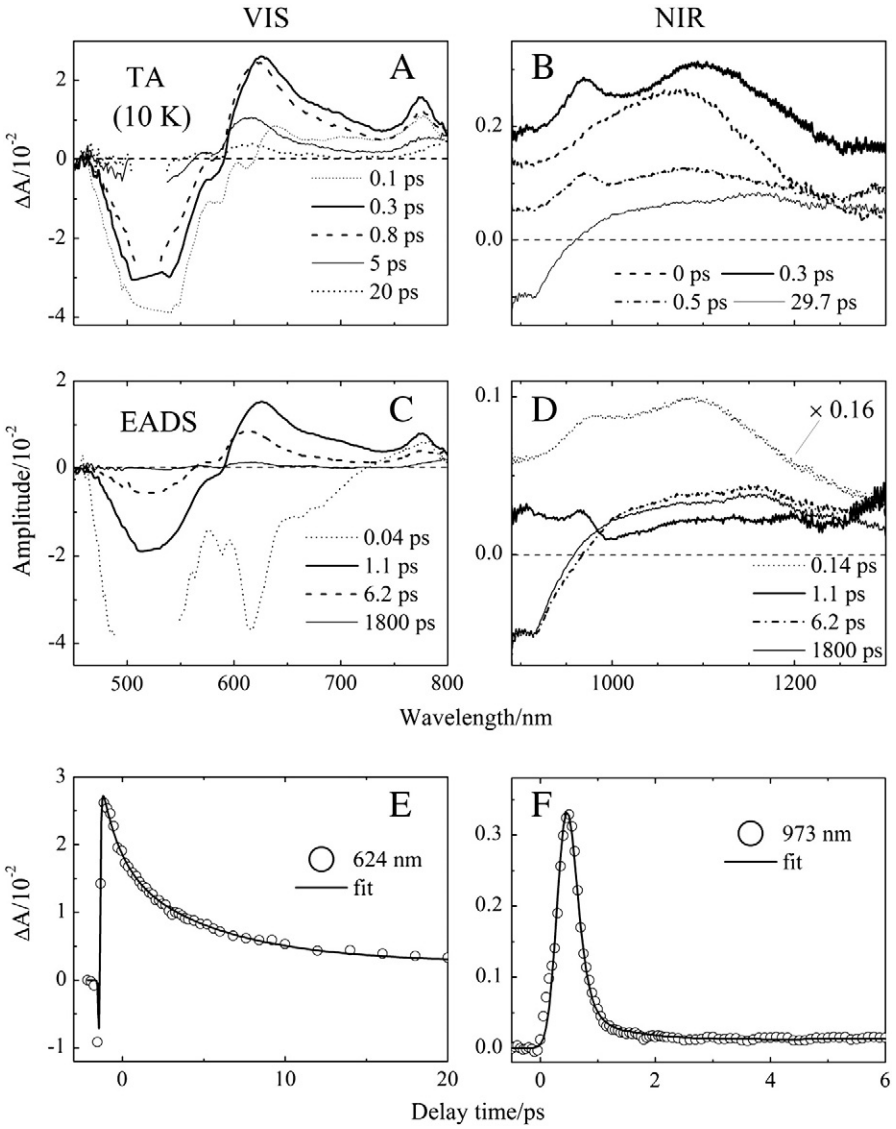

Fig. 6. (A, B) Low temperature (10 K) transient absorption spectra of the LH4 from *R. denitrificans* taken at different delay times in visible (VIS) and near-infrared (NIR) ranges in 50:50 (vol./vol.) glycerol/buffer. The LH4 complex was excited at 520 nm; (C–D) The results of global fitting of transient absorption datasets using sequential decay path (EADS). Fitting was done separately for VIS and NIR ranges; (E–F) The representative kinetics for VIS and NIR ranges extracted from the transient absorption data sets (circles) with corresponding fits obtained from global fitting analysis (solid lines).

but is red shifted by ~6 nm [26,27]. That places the maximum of the Q_y band of the "B850" ring at ~802 nm at RT.

The origin of the unique spectral properties of the B800–B820 complexes have been understood since the structures of the B800–B850 LH2 with its B800–B820 version (LH3) became available for comparison. It was concluded that the change of only two residues in the α-polypeptide is responsible for the spectral shift of the B850 band. In the B800–B850 complex from *Rps. acidophila*, orientation of the B850 molecules is maintained by a peptide that is coordinated with central magnesium ions via histidine residues (αHis31 with αBChl and βHis30 with βBChl) and by two α-polypeptide residues (αTyr44 and αThr45) forming hydrogen bonds (H-bonds) with the C3-acetyl group (ring A) of B850 molecules (αTyr44 with βB850 and αThr45 with αB850) [2]. In the case of the B800-B820 α-polypeptide, Tyr44 and Thr45 are replaced by Phe and Leu; both are unable to form H-bonds [6]. As a consequence, the H-bond pattern between protein and pigments changes and gives more freedom to the C3-acetyl groups of both α and βB820 BChl molecules and leads to de-planarity of the macrocycle and blue shift of the Q_y transition [28]. Recently, an influence of H-bonds on the spectroscopic properties was reported for the LH1 antenna complex from *Rdb. sphaeroides*, and these results strongly support this hypothesis [29].

The crystal structure of the peripheral light-harvesting complex from *R. denitrificans* is not yet available. However, the composition of α– and β-polypeptides can be projected based on the genome sequence and this is shown in Fig. 8 along with other known LH2 α– and β-polypeptide sequences. The shadowed area highlights residues responsible for the shift of the B850 band. The "standard" B800–B850 (LH2) complexes consist of α44, α45 amino acids with high H-bond affinity with the C3-acetyl group of B850 BChl: Tyr, Tyr (Y,Y) or Tyr, Trp (Y,W). In the B800–B820 complexes (LH3-like) these residues are replaced by amino acids like Phe and Leu that are unable to form H-bonds with the C3-acetyl group or ones with weak H-bond affinity like Thr. In the case of *R. denitrificans*, the situation is very similar, α44 and α45 residues are Phe and Leu. In addition, the residue next to Phe is aspartic acid, which with its negative character may cause an additional twist of the C3-acetyl group (to minimize repulsion between C=O groups). This should lead to a higher degree of macrocycle de-planarization and therefore induce a further blue shift of the Q_y transition. This explanation sounds reasonable; however, it is still only a hypothesis that will be settled when

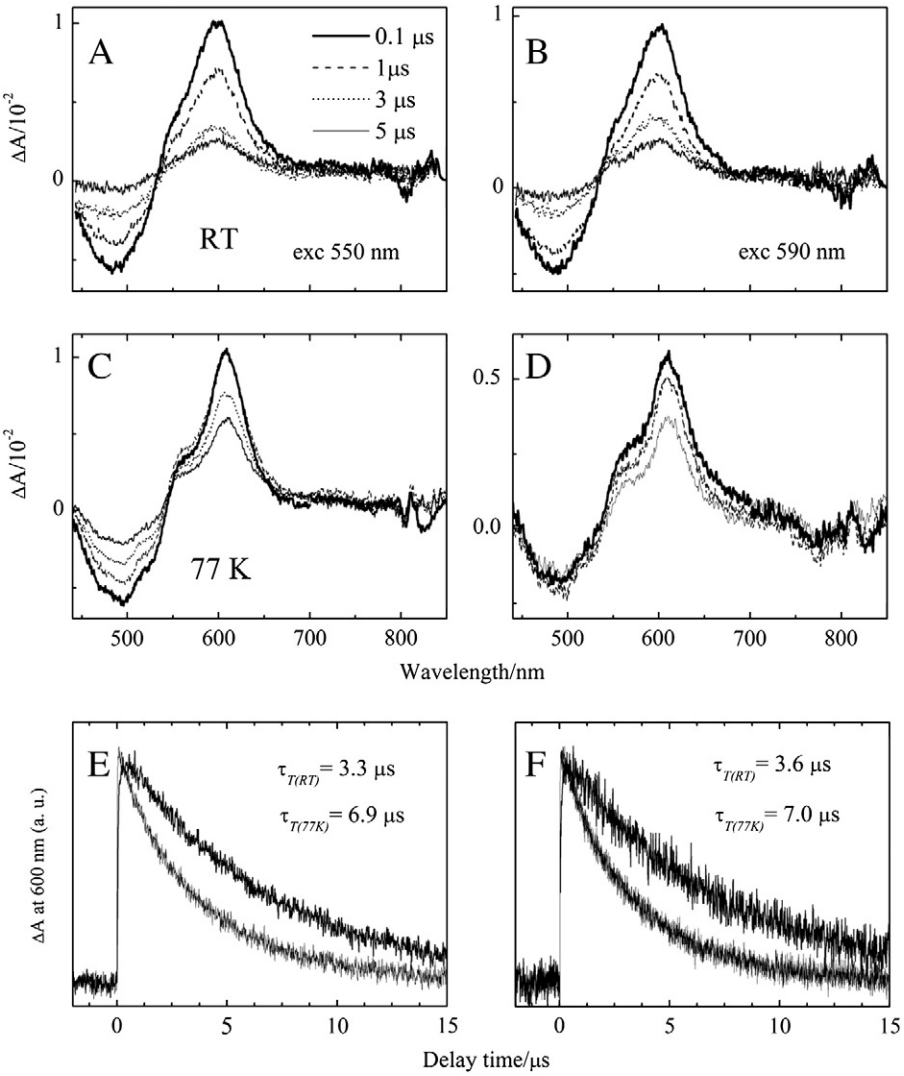

Fig. 7. (A, B) Room temperature and (C, D) low temperature (77 K) T–S spectra of the LH4 from *R. denitrificans* taken at different delay times in microsecond domain time. The samples were excited to the Car band (A, C) and to the BChl *a* Q_x band (B, D). (E, F) The Car triplet decay dynamics recorded at 600 nm. The spheroidenone triplet lifetime was obtained by monoexponential decay fitting of the measured kinetics. Carotenoid triplet lifetimes obtained from fitting are indicated in the figures.

the crystal structure becomes available. Moreover, the comparison of the group of α-polypeptides (Fig. 8) suggests that more peripheral light harvesting antenna complexes may have spectroscopic properties similar or even the same as the LH4 from *R. denitrificans*. These are LHCs from *Bradyrhizobium* sp. and *Dinoroseobacter shibae*. That conclusion cannot be confirmed at this point since the spectral properties of LHCs from these bacteria have not yet been characterized.

Interestingly, the LH4 from *R. denitrificans* has also an identical pigment composition as the LH2 from aerobically grown *Rdb. sphaeroides* (spheroidenone and BChl *a*) that has typical B800 and B850 bands. The spectroscopic properties and energy transfer in that LH2 were studied in detail before [30,31]. Such coincidence gives unique opportunity to understand how a spectral shift of the B850 band in the LH4 affects its photophysical properties in respect to the almost twin-like LH2 complex. Comparison of the steady-state absorption and fluorescence excitation profiles of both complexes reveals significant differences in the Car-to-BChl EET that from ~90% in the LH2 drops to ~70% in the LH4 studied here. It is clear that Car–BChl interaction is also affected.

The fluorescence lifetime of BChl *a* in the LH4 at both RT and 10 K is comparable to values obtained for the LH2 from *Rdb. sphaeroides*. In the LH2 it was measured to be 0.9–1 ns at RT and 1.3–1.8 ns at 6 K [32–36] compared to 0.63 ns (RT) and 1.8 ns (10 K) in the LH4 studied here. This demonstrates the relatively small influence of the B850 band shift on the photophysical properties of BChls bound to the protein.

Photophysical properties of spheroidenone were studied in two organic solvents (acetonitrile and *n*-hexane) and in LH2 [30,37]. In the present work, TA studies were performed in the highly polarizable solvent toluene (P(n) = 0.29) that mimics very well the steady-state absorption of spheroidenone natively bound to the LH2 or the LH4 complexes. The polarity of the chosen solvent was not important since this molecule, unlike other carbonyl Cars, does not demonstrate polarity-induced changes of the excited states lifetimes [37]. The S_1 ($2^1A_g^-$) state lifetime of 6.1 ps is in good agreement with the previously obtained value of 6 ps [37]. The spectral shape of the transient band is characteristic for nonpolar solvents and very well resembles the transient spectra obtained in *n*-hexane [37]. The TA spectra of spheroidenone bound to the LH4 (Fig. 5) are flatter and broader likely due to increase of protein mediated polarity. The kinetic components lifetimes obtained at RT are very comparable to those obtained for the LH2 and can be clearly assigned to the different excited states. The 100 fs component is associated with the $S_2(1^1B_u^+)$ state. The lifetime is slightly shorter than intrinsic (120 fs) and suggests additional depleting of the state by energy transfer to BChls. The second component with lifetime of 0.78 ps has the spectral shape typical for the $S_1(2^1A_g^-) \rightarrow S_n$ transient

α-polypeptide

```
                                    ....|....| ....|....| ....|....| ....|....| ....|....| ....|....| ....|....|
                                             10         20         30         40         50         60
B800-B850 Rba. spha 2.4.1           MTNGKIWLVV KPTVGVPLFL SAAVIASVVI HAAVLTTTTW LPAYYQGSAA VAAE......
B800-B850 Rba. spha ATCC 17029      MTNGKIWLVV KPTVGVPLFL SAAVIASVVI HAAVLTTTTW LPAYYQGSAA VAAE......
B800-B850 Rba. spha KD131           MTNGKIWLVV KPTVGVPLFL SAAVIASVVI HAAVLTTTTW LPAYYQGSAA VAAE......
B800-B850 Rps. acidop 7750          MNQGKIWTVV NPAIGIPALL GSVTVIAILV HLAILSHTTW FPAYWQGVKK ..........
B800-B850 Rps. acid 7050            MNQGKIWTVV NPSVGLPLLL GSVTVIIALV HAAVLSHTTW FPAYWQGGLK K.........
B800-B850 Rps. acid 10050           MNQGKIWTVV NPAIGIPALL GSVTVIAILV HLAILSHTTW FPAYWQGGVK K.........
B800-B850 Rps. pal CGA009 chA       MNQARIWTVV KPTVGLPLLL GSVTVIAILV HFAVLSHTTW FSKYWNGKAA AIESSVNVG.
B800-B850 Rps. pal CGA009 chE       MNQGRIWTVV KPTVGLPLLL GSVTVIAILV HFAVLSNTTW FSKYWNGKAA AIESSVSIG.
B800-B850 Rps. pal CGA009 chB       MNQGRIWTVV NPGVGLPLLL GSVTVIAILV HYAVLSNTTW FPKYWNGATV AAPAAAPAPA
B800-B850 Rba. cap SB 1003          MNNAKIWTVV KPSTGIPLIL GAVAVAALIV HAGLLTNTTW FANYWNGNPM ATVVAVAPAQ
B800-B850 Bradyr sp. BTAi1          MNQGRIWCVV NPTVGLPLFL GSVALTSLCV HYTVLTHTTW MGAFFEGGKS KKASLEETVS
B800-B850 Rps. pal CGA009 chD       MNQGRIWTVV KPTVGLPLLL GSVAIMVFLV HFAVLTHTTW VAKFMNGKAA AIESSIKAV.
B800-B820 Rps. acid 7750            MNQGKIWTVV NPAVGLPLLL G-SVAITALV HLAVLTHTTW FPAFTQGGLK K.........
B800-B820 Rps. acid 7050            MNQGKIWIVV PPAFGLPLML GAVAITALLV HAAVLTHTTW YAAFLQGGVK K.........
B8?? Dino shibae DFL 12             MNNAKMWLVV PPAVGVPVFL GAVAVGSFAV HVAVLSNTSW VSDFLSGNEL GSGDSAALLQ
B800 Roseo denit OCh 114            MNNAKMWLVV SPSVGVPVFL GAVAVGSFAV HVAVLSNTSW VSDFLSGNEL GSGDAQEAAA

                                    ....|....| ....|....| ....|....| ....|....| ....|....| ....|....| ....|....|
                                             70         80         90        100        110        120
B800-B850 Rba. spha 2.4.1           .......... .......... .......... .......... .......... ..........
B800-B850 Rba. spha ATCC 17029      .......... .......... .......... .......... .......... ..........
B800-B850 Rba. spha KD131           .......... .......... .......... .......... .......... ..........
B800-B850 Rps. acidop 7750          .......... .......... .......... .......... .......... ..........
B800-B850 Rps. acid 7050            .......... .......... .......... .......... .......... ..........
B800-B850 Rps. acid 10050           .......... .......... .......... .......... .......... ..........
B800-B850 Rps. pal CGA009 chA       .......... .......... .......... .......... .......... ..........
B800-B850 Rps. pal CGA009 chE       .......... .......... .......... .......... .......... ..........
B800-B850 Rps. pal CGA009 chB       APAAKK.... .......... .......... .......... .......... ..........
B800-B850 Rba. cap SB 1003          .......... .......... .......... .......... .......... ..........
B800-B850 Bradyr sp. BTAi1          PVALNAKAVP GYVISVAPVS AENARAGSSF VVTVAPVPAQ AQATSEDTTS HAPDKVSLAT
B800-B850 Rps. pal CGA009 chD       .......... .......... .......... .......... .......... ..........
B800-B820 Rps. acid 7750            .......... .......... .......... .......... .......... ..........
B800-B820 Rps. acid 7050            .......... .......... .......... .......... .......... ..........
B8?? Dino shibae DFL 12             QQEAATAKAS YVLPDVNGAQ QVLIVMPDGT TRTAVLQGET LASASPTVPP SSY.......
B800 Roseo denit OCh 114            RILENADNDV ANASYVVPSA DGSQQVLVVM PDGTTAMATL QSPSYVQASV TQPVTIEQ..
```

β-polypeptide

```
                                    ....|....| ....|....| ....|....| ....|....| ....|....| ..
                                             10         20         30         40         50
B800-B850 Rba. spha 2.4.1           -MTDDLNKVW PSGLTVAEAE EVHKQLILGT RVFGGMALIA HFLAAAATPW LG
B800-B850 Rba. spha ATCC 17029      -MTDDLNKVW PSGLTVAEAE EVHKQLILGT RVFGGMALIA HFLAAAATPW LG
B800-B850 Rba. spha KD131           -MTDDPKKVW PSGLTIAEAE EVHKQLILGT RVFGGMALIA HFLAAAATPW LG
B800-B850 Rps. acidop 7750          --A------- --TLTAEQSE ELHKYVIDGT RVFLGLALVA HFLAFSATPW LH
B800-B850 Rps. acid 7050            --ADDV-K-G LTGLTAAESE ELHKHVIDGT RVFFVIAIFA HVLAFAFSPW LH
B800-B850 Rps. acid 10050           --A------- -TLTAEQQSE ELHKYVIDGT RVFLGLA-VA HFLAFSATPW LH
B800-B850 Rps. pal CGA009 chA       -MAD---K-T LTGLTVEESE ELHKHVIDGT RIFGAIAIVA HFLAYVYSPW LH
B800-B850 Rps. pal CGA009 chE       -MADDPNKVW PTGLTIAESE ELHKHVIDGT RIFGAIAIVA HFLAYVYSPW LH
B800-B850 Rps. pal CGA009 chB       -MADDPNKVW PTGLTIAESE ELHKHVIDGT RIFGAIAIVA HFLAYVYSPW LH
B800-B850 Rba. cap SB 1003          -MTDD--KAG PSGLSLKEAE EIHSYLIDGT RVFGAMALVA HILSAIATPW LG
B800-B850 Bradyr sp. BTAi1          MMPDDPNRVW PTGLTIPESE ELHKHVIDGA RVFFVIACVA HLLAYIYSPW LH
B800-B850 Rps. pal CGA009 chD       -MVDDPNKVW PTGLTIAESE ELHKHVIDGS RIFVAIAIVA HFLAYVYSPW LH
B800-B820 Rps. acid 7750            --AD---K-- P--LTADQAE ELHKYVIDGA RAFVAIAAFA HVLAYSLTPW LH
B800-B820 Rps. acid 7050            --A------- -EVLTSEQAE ELHKHVIDGT RVFLVIAAIA HFLAFTLTRW LH
B8?? Dino shibae DFL 12             -MADDTDKVW PTGLTLEEAE EVHSYLIDGT RVFGVIALLA HFLVAAATPW LG
B800 Roseo denit OCh 114            -MSDDPDKVW PTGLTLLEAE EVHSYLIDGT RVFGAIALVA HMLVAASTPW LG
```

Fig. 8. Comparison of α- and β-apoprotein sequences from a collection of peripheral light harvesting complexes from different photosynthetic purple bacteria species and strains. The sequences were obtained from National Center for Biotechnology Information (NCBI). Rba. spha—*Rhodobacter sphaeroides*, Rps. acid—*Rhodopseudomonas acidophila*, Rps. pal—*Rhodopseudomonas palustris*, Rba. cap—*Rhodobacter capsulatus*, Bradyr sp.—*Bradyrhizobium* sp., Dino shibae—*Dinoroseobacter shibae*, Roseo denit—*Roseobacter denitrificans*. The part of sequence in which sequence differences are responsible for the blue shift of the B850 band is marked in gray.

band and is associated with decay of the $S_1(2^1A_g^-)$ state. Lifetime shortening illustrates that the state is significantly depleted by processes additional to internal conversion. The third component (5.1 ps) is more difficult to understand. It has shape and lifetime very similar to those observed for the Car $S_1(2^1A_g^-) \rightarrow S_n$ transition in toluene. It may suggest that some fraction of the Car is very weakly bound to the complex and does not participate in energy transfer to BChl *a*. That is a reasonable explanation for the low Car-to-BChl EET (70%) compared to the spheroidenone-containing LH2. This hypothesis seems to be even more likely if we compare global fitting results of TA of the LH4 and the LH2 from Cong et al. [30]. The kinetic component with lifetime of ~5 ps is present in both complexes; however its amplitude is around 2 times smaller than in the LH4 in respect to the main $S_1(2^1A_g^-) \rightarrow S_n$ transient band. The last kinetic component with lifetime of ~600 ps has no Car signature and is entirely associated with BChl *a* transient bands. In the NIR range (Fig. 5D) along with the expected spectral features already seen in spheroidenone NIR data in toluene, a new kinetic component with lifetime of 0.75 ps is observed. It contains a band with maximum at 968 nm that was previously assigned to the $D_0 \rightarrow D_2$ TA of Car radical cation ($Car^{+\bullet}$) and was recorded in a series of LH2 complexes containing different Cars as well as predicted theoretically [30,31,38,39]. In LH2 complexes $Car^{+\bullet}$ can be formed only upon direct excitation of Car S_2 $(1^1B_u^+)$ state via formation of Car–B800 intermolecular charge transfer state [38–40]. Since observable spectral features are associated with a ground-state spectrum of $Car^{+\bullet}$, the measured lifetime represents the rate of charge recombination between $Car^{+\bullet}$ and the B800 anion. For both, the spheroidenone containing LH2 and the LH4 charge recombination time is fast, shorter by 10 times or more compared to other Cars

in LH2 complexes [30,38,40]. The importance of $Car^{+\bullet}$ formation in LH2s seems to be negligible since only a few present of excited Car molecules is converted [30]. A similar situation is observed in the LH4 from this work. Amplitude of the $D_0 \rightarrow D_2$ band is ~10 times smaller compared to the amplitude of the initial $S_0(1^1A_g^-) \rightarrow S_2(1^1B_u^+)$ bleaching. The extinction coefficients of both transitions are comparable for Cars [41] and the yield of spheroidenone radical cation formation in the LH4 can be assumed to ~10%.

In their recent studies of TA of stable $Car^{+\bullet}$ (lutein and β-carotene), Amarie et al. [42] pointed out that a D_2 state (D_3 in Amarie's notation) with its large oscillator strength can serve as a (B)Chls energy acceptor. Since $Car^{+\bullet}$ exists for only a few picoseconds in its ground state in LH2 complexes, $Q_y(B850) \rightarrow D_2$ energy transfer should occur within this time frame. As a result of the ET process, we should observe bleaching of the $D_0 \rightarrow D_2$ band coupled with the $D_2 \rightarrow D_n$ and subsequently the $D_1 \rightarrow D_n$ transient absorption bands. Based on Amarie's results, these should decay in the picosecond time scale. So far, none of these processes have been observed in the TA of the LH2s or in the LH4. Even if energetically this process is favorable, the required spectral overlap between the BChl *a* Q_y emission and the $D_0 \rightarrow D_2$ $Car^{+\bullet}$ absorption is practically zero due to the large energetic distance between both transitions. In addition, functioning of the proposed mechanism will require a sequential photon absorption by the same carotenoid molecule (first to form a $Car^{+\bullet}$ and second to excite it to the D_2 state) within few picoseconds. This is impossible under ambient light in natural condition, though it may happen upon excitation with high photon densities provided by laser.

Taking the sample to very low temperature marginally affects the Car kinetic components and only a small increase in the $S_1(1^1A_g^-)$ singlet state lifetimes is observed. Also, the transient spectra become a bit more resolved, but overall they show the same properties as those taken at RT. Interestingly, some spectra shift to longer wavelengths compared to the RT results. The $S_1(1^1A_g^-) \rightarrow S_n$ transient band is shifted by 15 nm (610 nm peak shifts to 625 nm) while the $S_2(1^1B_u^+) \rightarrow S_n$ band became wider and demonstrate too maxima at 970 and 1090 nm. The $Car^{+\bullet}$ $D_0 \rightarrow D_2$ remains the same. This effect has not been observed previously for spheroidenone in the LH2 [30]. The simplest explanation is that low temperature affects the immediate environment of spheroidenone by changing (increasing) its refractive index and therefore its polarizability. Increasing polarizability will stabilize B_u-like singlet excited states energies (including the $S_2(1^1B_u^+)$ state) but will not affect excited singlet state energies with A_g-like character (including the $S_1(1^1A_g^-)$ state). Since both, the $A_g \rightarrow B_u$ and $B_u \rightarrow A_g$ transitions are manifested in TA, they will be affected, however in the opposite way. The $A_g \rightarrow B_u$ transitions will have smaller energies afterward (red shift) while $B_u \rightarrow A_g$ larger (blue shift). It may look that the $S_2(1^1B_u^+) \rightarrow S_n$ band does not follow the rule however such wide and vibrationless spectrum either at RT and at 10 K prohibits undeniably define positions and amplitudes of vibronic bands and how they change and shift upon lowering temperature. Moreover, the same effect should also be observed in the 10 K LH4 steady-state absorption spectrum, but due to the vibronicless structure of spheroidenone absorption spectrum it is difficult to detect. This effect suggests that spheroidenone molecules are not so well wrapped by polypeptides in the LH4 complex and are more exposed to the environment surrounding the complex compared to their counterparts in LH2.

Spectroscopic studies of Cars triplet state in LH2, LH1 antenna complexes and in RCs were performed for several molecules [43–47]. The RT triplet transient band of spheroidenone in the LH4 complex does not show vibronic features and appears as a single broad band. Low temperature (77 K) does not improve resolution and only a slight narrowing of the band is observed. Based on comparison of the T–S profiles and the TA spectra of the LH4 from the pico- and nanosecond scale, it is clear that the entire pool of spheroidenone triplets is populated via quenching of BChl *a* triplets. Intramolecular intersystem crossing does not participate in Car triplet formation; otherwise a T–S spectral signature should be visible also in TA on the subnanosecond time scale. Based on the studies of conjugation length dependence of Car triplet lifetime in different LH2 complexes [45], ~5 μs triplet lifetime is expected for this Car in the LH2 or in the LH4 at RT. The obtained value of 3.3–3.6 μs is lower, but the difference can be easily accounted for as the effect of either a result of quenching by residual molecular oxygen or a Car concentration-dependent self-quenching process [48]. The T–S spectral profiles reveal also very weak negative bands at ~800 nm (RT) and 820 nm (77 K) corresponding very well to the expected position of the Q_y band of BChls (Fig. 8C). Similar spectroscopic features, so called "interaction bands" were observed in LH2 complexes and are interpreted as a small delocalization of the Car triplet wave function over an adjacent BChl *a* molecule [43,49]. For the LH2 complex from *Rdb. sphaeroides*, only one interaction band in the 850 nm region was detected, indicating predominant interaction of the Car triplet with longer wavelength BChl *a* [43]. In the LH4 complex studied here, two interaction bands at 800 and 820 have equal intensities; however they are still very weak compared to the $T_1 \rightarrow T_n$ Car band (Fig. 8C).

5. Conclusions

A peripheral light-harvesting complex from the aerobic purple bacterium *R. denitrificans* demonstrates unique spectroscopic properties. Circular dichroism and low temperature steady-state absorption spectroscopy revealed that the B850 band is present but is shifted significantly to shorter wavelengths and overlaps with the B800 band at room temperature. The spectroscopic properties classify this protein to the LH4 class of peripheral light-harvesting complexes, along with the previously known LH4 from *Rhodopseudomonas palustris*. The same pigment compositions of the LH4 from *R. denitrificans* and the LH2 from aerobically grown *Rb. sphaeroides* allowed us to compare both antenna complexes and understand how the specific changes in the structural and spectroscopic properties affect efficiency of energy transfer between pigments within the protein.

Acknowledgments

This material is based upon a work supported as part of the Photosynthetic Antenna Research Center (PARC), an Energy Frontier Research Center funded by the U.S. Department of Energy, Office of Science, Office of Basic Energy Sciences under Award Number DE-SC 0001035. Work in the laboratory of HAF was supported by grants from the National Science Foundation (MCB-0913022) and the University of Connecticut Research Foundation.

References

[1] A.R. Grossman, D. Bhaya, K.E. Apt, D.M. Kehoe, Light-harvesting complexes in oxygenic photosynthesis: diversity, control, and evolution, Annu. Rev. Genet. 29 (1995) 231–288.
[2] G. Mcdermott, S.M. Prince, A.A. Freer, A.M. Hawthornthwaitelawless, M.Z. Papiz, R.J. Cogdell, N.W. Isaacs, Crystal structure of an integral membrane light-harvesting complex from photosynthetic bacteria, Nature 374 (1995) 517–521.
[3] S.M. Prince, M.Z. Papiz, A.A. Freer, G. McDermott, A.M. Hawthornthwaite-Lawless, R.J. Cogdell, N.W. Isaacs, Apoprotein structure in the LH2 complex from *Rhodopseudomonas acidophila* strain 10050: modular assembly and protein pigment interactions, J. Mol. Biol. 268 (1997) 412–423.
[4] M.Z. Papiz, S.M. Prince, T. Howard, R.J. Cogdell, N.W. Isaacs, The structure and thermal motion of the B800-850 LH2 complex from *Rps. acidophila* at 2.0 Å resolution and 100 K: new structural features and functionally relevant motions, J. Mol. Biol. 326 (2003) 1523–1538.
[5] J. Koepke, X. Hu, C. Muenke, K. Schulten, H. Michel, The crystal structure of the light-harvesting complex II (B800-850) from *Rhodospirillum molischianum*, Structure 4 (1996) 581–597.
[6] K. McLuskey, S.M. Prince, R.J. Cogdell, N.W. Isaacs, The crystallographic structure of the B800-820 LH3 light-harvesting complex from the purple bacteria *Rhodopseudomonas acidophila* strain 7050, Biochem.-Us 40 (2001) 8783–8789.
[7] R.J. Cogdell, A.M. Hawthornthwaite, M.B. Evans, L.A. Ferguson, C. Kerfeld, J.P. Thornber, F. Vanmourik, R. Vangrondelle, Isolation and characterization of an unusual antenna complex from the marine purple sulfur photosynthetic

bacterium *Chromatium purpuratum* BN5500, Biochim. Biophys. Acta 1019 (1990) 239–244.
[8] J.P. Thornber, Photochemical reactions of purple bacteria as revealed by studies of three spectrally different carotenobacteriochlorophyll–protein complexes isolated from *Chromatium*, strain D, Biochem.-Us 9 (1970) 2688–2698.
[9] N. Hartigan, H.A. Tharia, F. Sweeney, A.M. Lawless, M.Z. Papiz, The 7.5 Å electron density and spectroscopic properties of a novel low-light B800 LH2 from *Rhodopseudomonas palustris*, Biophys. J. 82 (2002) 963–977.
[10] K. Shimada, H. Hayashi, T. Noguchi, M. Tasumi, Excitation and emission-spectroscopy of membranes and pigment-protein complexes of an aerobic photosynthetic bacterium, *Erythrobacter* sp OCh 114, Plant Cell Physiol. 31 (1990) 395–398.
[11] K. Shimada, I. Yamazaki, N. Tamai, M. Mimuro, Excitation-energy flow in a photosynthetic bacterium lacking B850—fast energy-transfer from B806 to B870 in *Erythrobacter* sp strain OCh 114, Biochim. Biophys. Acta 1016 (1990) 266–271.
[12] D.M. Niedzwiedzki, A.M. Collins, A.M. LaFountain, M.M. Enriquez, H.A. Frank, R.E. Blankenship, Spectroscopic studies of carotenoid-to-bacteriochlorophyll energy transfer in LHRC photosynthetic complex from *Roseiflexus castenholzii*, J. Phys. Chem. B 114 (2010) 8723–8734.
[13] R.P. Ilagan, R.L. Christensen, T.W. Chapp, G.N. Gibson, T. Pascher, T. Polivka, H.A. Frank, Femtosecond time-resolved absorption spectroscopy of astaxanthin in solution and in alpha-crustacyanin, J. Phys. Chem. A 109 (2005) 3120–3127.
[14] D.M. Niedzwiedzki, R.E. Blankenship, Singlet and triplet excited state properties of natural chlorophylls and bacteriochlorophylls, Photosynth. Res. 106 (2010) 227–238.
[15] E.L. Read, G.S. Schlau-Cohen, G.S. Engel, T. Georgiou, M.Z. Papiz, G.R. Fleming, Pigment organization and energy level structure in light-harvesting complex 4: insights from two-dimensional electronic spectroscopy, J. Phys. Chem. B 113 (2009) 6495–6504.
[16] A.T. Gardiner, S. Takaichi, R.J. Cogdell, The effect of changes in light intensity and temperature on the peripheral antenna of *Rhodopseudomonas acidophila*, Biochem. Soc. Trans. 21 (1993) 6S.
[17] M. Gabrielsen, A.T. Gardiner, R. Cogdell, Peripheral complexes of purple bacteria, in: C.N. Hunter, F. Daldal, M.C. Thurnauer, J.T. Beatty (Eds.), The Purple Phototrophic Bacteria, Springer, Dordrecht, 2009, pp. 135–153.
[18] D.M. Niedzwiedzki, J.O. Sullivan, T. Polivka, R.R. Birge, H.A. Frank, Femtosecond time-resolved transient absorption spectroscopy of xanthophylls, J. Phys. Chem. B 110 (2006) 22872–22885.
[19] D. Niedzwiedzki, J.F. Koscielecki, H. Cong, J.O. Sullivan, G.N. Gibson, R.R. Birge, H.A. Frank, Ultrafast dynamics and excited state spectra of open-chain carotenoids at room and low temperatures, J. Phys. Chem. B 111 (2007) 5984–5998.
[20] T. Polivka, V. Sundstrom, Dark excited states of carotenoids: consensus and controversy, Chem. Phys. Lett. 477 (2009) 1–11.
[21] T. Polivka, V. Sundstrom, Ultrafast dynamics of carotenoid excited states—from solution to natural and artificial systems, Chem. Rev. 104 (2004) 2021–2071.
[22] H.A. Frank, R.Z.B. Desamero, V. Chynwat, R. Gebhard, I. vanderHoef, F.J. Jansen, J. Lugtenburg, D. Gosztola, M.R. Wasielewski, Spectroscopic properties of spheroidene analogs having different extents of p-electron conjugation, J. Phys. Chem. A 101 (1997) 149–157.
[23] P.O. Andersson, R.J. Cogdell, T. Gillbro, Femtosecond dynamics of carotenoid-to-bacteriochlorophyll a energy transfer in the light-harvesting antenna complexes from the purple bacterium *Chromatium purpuratum*, Chem. Phys. 210 (1996) 195–217.
[24] D.M. Niedzwiedzki, M.M. Enriquez, A.M. LaFountain, H.A. Frank, Ultrafast time-resolved absorption spectroscopy of geometric isomers of xanthophylls, Chem. Phys. 373 (2010) 80–89.
[25] I.H. van Stokkum, D.S. Larsen, R. van Grondelle, Global and target analysis of time-resolved spectra, Biochim. Biophys. Acta 1657 (2004) 82–104.
[26] S. Georgakopoulou, R.N. Frese, E. Johnson, C. Koolhaas, R.J. Cogdell, R. van Grondelle, G. van der Zwan, Absorption and CD spectroscopy and modeling of various LH2 complexes from purple bacteria, Biophys. J. 82 (2002) 2184–2197.
[27] V. Sundstrom, T. Pullerits, R. van Grondelle, Photosynthetic light-harvesting: reconciling dynamics and structure of purple bacterial LH2 reveals function of photosynthetic unit, J. Phys. Chem. B 103 (1999) 2327–2346.
[28] E. Gudowskanowak, M.D. Newton, J. Fajer, Conformational and environmental-effects on bacteriochlorophyll optical–spectra-correlations of calculated spectra with structural results, J. Phys. Chem.-Us 94 (1990) 5795–5801.
[29] G. Uyeda, J.C. Williams, M. Roman, T.A. Mattioli, J.P. Allen, The Influence of hydrogen bonds on the electronic structure of light-harvesting complexes from photosynthetic bacteria, Biochem.-Us 49 (2010) 1146–1159.
[30] H. Cong, D.M. Niedzwiedzki, G.N. Gibson, A.M. LaFountain, R.M. Kelsh, A.T. Gardiner, R.J. Cogdell, H.A. Frank, Ultrafast time-resolved carotenoid to-bacteriochlorophyll energy transfer in LH2 complexes from photosynthetic bacteria, J. Phys. Chem. B 112 (2008) 10689–10703.
[31] T. Polivka, T. Pullerits, H.A. Frank, R.J. Cogdell, V. Sundstrom, Ultrafast formation of a carotenoid radical in LH2 antenna complexes of purple bacteria, J. Phys. Chem. B 108 (2004) 15398–15407.
[32] A. Freiberg, M. Ratsep, K. Timpmann, G. Trinkunas, N.W. Woodbury, Self-trapped excitons in LH2 antenna complexes between 5 K and ambient temperature, J. Phys. Chem. B 107 (2003) 11510–11519.
[33] M.A. Bopp, Y.W. Jia, L.Q. Li, R.J. Cogdell, R.M. Hochstrasser, Fluorescence and photobleaching dynamics of single light-harvesting complexes, Proc. Natl Acad. Sci. U.S.A. 94 (1997) 10630–10635.
[34] T. Pflock, M. Dezi, G. Venturoli, R.J. Cogdell, J. Kohler, S. Oellerich, Comparison of the fluorescence kinetics of detergent-solubilized and membrane-reconstituted LH2 complexes from *Rps. acidophila* and *Rb. sphaeroides*, Photosynth. Res. 95 (2008) 291–298.
[35] R. Monshouwer, M. Abrahamsson, F. vanMourik, R. vanGrondelle, Superradiance and exciton delocalization in bacterial photosynthetic light-harvesting systems, J. Phys. Chem. B 101 (1997) 7241–7248.
[36] X.H. Chen, L. Zhang, Y.X. Weng, L.C. Du, M.P. Ye, G.Z. Yang, R. Fujii, F.S. Rondonuwu, Y. Koyama, Y.S. Wu, J.P. Zhang, Protein structural deformation induced lifetime shortening of photosynthetic bacteria light-harvesting complex LH2 excited state, Biophys. J. 88 (2005) 4262–4273.
[37] D. Zigmantas, R.G. Hiller, F.P. Sharples, H.A. Frank, V. Sundstrom, T. Polivka, Effect of a conjugated carbonyl group on the photophysical properties of carotenoids, Phys. Chem. Chem. Phys. 6 (2004) 3009–3016.
[38] T. Polivka, D. Zigmantas, J.L. Herek, Z. He, T. Pascher, T. Pullerits, R.J. Cogdell, H.A. Frank, V. Sundstrom, The carotenoid S_1 state in LH2 complexes from purple bacteria *Rhodobacter sphaeroides* and *Rhodopseudomonas acidophila*: S_1 energies, dynamics, and carotenoid radical formation, J. Phys. Chem. B 106 (2002) 11016–11025.
[39] M. Wormit, A. Dreuw, Carotenoid radical cation formation in LH2 of purple bacteria: a quantum chemical study, J. Phys. Chem. B 110 (2006) 24200–24206.
[40] T. Polivka, D. Niedzwiedzki, M. Fuciman, V. Sundstrom, H.A. Frank, Role of B800 in carotenoid-bacteriochlorophyll energy and electron transfer in LH2 complexes from the purple bacterium *Rhodobacter sphaeroides*, J. Phys. Chem. B 111 (2007) 7422–7431.
[41] J.A. Jeevarajan, C.C. Wei, A.S. Jeevarajan, L.D. Kispert, Optical absorption spectra of dications of carotenoids, J. Phys. Chem.-Us 100 (1996) 5637–5641.
[42] S. Amarie, K. Arefe, J.H. Starcke, A. Dreuw, J. Wachtveitl, Identification of an additional low-lying axcited state of carotenoid radical cations, J. Phys. Chem. B 112 (2008) 14011–14017.
[43] A. Angerhofer, F. Bornhauser, A. Gall, R.J. Cogdell, Optical and optically detected magnetic-resonance investigation on purple photosynthetic bacterial antenna complexes, Chem. Phys. 194 (1995) 259–274.
[44] J. Feng, Q. Wang, Y.S. Wu, X.C. Ai, X.J. Zhang, Y.G. Huang, X.K. Zhang, J.P. Zhang, Triplet excitation transfer between carotenoids in the LH2 complex from photosynthetic bacterium *Rhodopseudomonas palustris*, Photosynth. Res. 82 (2004) 83–94.
[45] Y. Kakitani, J. Akahane, H. Ishii, H. Sogabe, H. Nagae, Y. Koyama, Conjugation-length dependence of the T-1 lifetimes of carotenoids free in solution and incorporated into the LH2, LH1, RC, and RC-LH1 complexes: possible mechanisms of triplet-energy dissipation, Biochem.-Us 46 (2007) 2181–2197.
[46] H.A. Frank, B.W. Chadwick, S. Taremi, S. Kolaczkowski, M.K. Bowman, Singlet and triplet absorption spectra of carotenoids bound in the reaction centers of *Rhodobacter sphaeroides* R26, FEBS Lett. 203 (1986) 157–163.
[47] H.A. Frank, J. Machnicki, M. Felber, Carotenoid triplet states in photosynthetic bacteria, Photochem. Photobiol. 35 (1982) 713–718.
[48] M. Burke, E.J. Land, D.J. McGarvey, T.G. Truscott, Carotenoid triplet state lifetimes, J. Photoch. Photobiol. B 59 (2000) 132–138.
[49] D.M. Niedzwiedzki, M. Kobayashi, R.E. Blankenship, Triplet excited state spectra and dynamics of carotenoids from the thermophilic purple photosynthetic bacterium *Thermochromatium tepidum*, Photosynth. Res. 107 (2) (2011) 177–186.